Quantum plasmonic sensing

Wenjiang Fan,[1,2] Benjamin J. Lawrie,[2] and Raphael C. Pooser[2,*]
[1]*Department of Physics, University of Virginia, Charlottesville, Virginia 22903, USA*
[2]*Quantum Information Science Group, Oak Ridge National Laboratory, Oak Ridge, Tennessee 37830, USA*
(Received 18 June 2015; published 4 November 2015)

Surface plasmon resonance (SPR) sensors can reach the quantum noise limit of the optical readout field in various configurations. We demonstrate that two-mode intensity squeezed states produce a further enhancement in sensitivity compared with a classical optical readout when the quantum noise is used to transduce an SPR sensor signal in the Kretschmann configuration. The quantum noise reduction between the twin beams when incident at an angle away from the plasmonic resonance, combined with quantum noise resulting from quantum anticorrelations when on resonance, results in an effective SPR-mediated modulation that yields a measured sensitivity 5 dB better than that with a classical optical readout in this configuration. The theoretical potential of this technique points to resolving particle concentrations with more accuracy than is possible via classical approaches to optical transduction.

DOI: 10.1103/PhysRevA.92.053812 PACS number(s): 42.50.Lc, 07.07.Df, 73.20.Mf, 42.50.Dv

I. INTRODUCTION

Caves first proposed the idea of using quantum noise reduction in sensors in 1981 [1]. The concept works by directly reducing the noise sidebands in a measurement, which thereby allows one to detect smaller phenomena that would otherwise have been lost in the shot noise. However, due to the optical loss associated with most practical systems, which destroys quantum noise reduction, quantum sensing remained un unfulfilled promise of quantum optics for decades. Recently, devices have been engineered to reduce loss to the point that quantum sensing is possible in several scenarios [2–7]. However, these have typically been specialized applications and have always required minimal optical losses. Here, we simultaneously take advantage of both quantum noise reduction and the optical losses in a ubiquitous Kretschmann surface plasmon resonance (SPR) sensor in order to provide a 5-dB improvement in sensitivity compared to the classical analog. The implementation demonstrates application of quantum noise reduction to the most widely used sensor platform yet, increasing the reach of quantum sensors to myriad other disciplines while providing the most accessible quantum sensing configuration available to date.

SPR sensors have been studied for decades because of their high sensitivity that results from nanoscale electric-field confinement [8–14]. With recent advances in chemical functionalization and nanofabrication, label-free chemical and biological plasmonic sensors have become widely available in recent years [15,16]. However, the sensitivity of SPR sensors is fundamentally limited by the Heisenberg uncertainty of the optical readout light: the shot-noise limit (SNL) [17]. Phase-based SPR sensors have demonstrated an order of magnitude improvement in sensitivity compared with intensity-based sensors [18,19], but they too are ultimately limited by the quantum statistics of light.

Recent letters [20,21] have shown that localized and propagating surface plasmons can coherently transduce squeezed states, pointing to the possibility of quantum plasmonic sensors capable of surpassing the shot-noise limit. Demonstrations of the Hong-Ou-Mandel effect in plasmonic media [22,23] have also proved that plasmons can behave as bosons, which preserve and transmit quantum states and quantum information effectively. In addition, recent work [24] has enabled observation of a refractive-index change of $\Delta n = 0.014$ by detecting coincidences of single photons above an *ad hoc* added excess background noise. However, typical SPR sensors utilize optical readout powers ranging from tens of microwatts to tens of milliwatts in order to minimize the effect of shot noise, without turning the power so high as to damage photosensitive elements or thermally modulate the sensor itself. The sensor we outline here utilizes bright quantum states of light with milliwatt-level power to achieve sensitivity more than an order of magnitude better than any previous device that utilizes quantum states. The same enhancement can be seen under excess noise conditions, such as relatively large electronics noise on resonance in the present system, since the quantum correlations themselves serve as a strong filter that rejects background noise. Thus, the sensor provides all of the benefits of a single-photon, coincidence-counting readout with the additional advantages of tunable, bright fields for increased sensitivity.

II. EXPERIMENTAL DESIGN

Two-mode squeezed light, generated via four-wave mixing (4WM) [25] in Rb vapor, has shown promise for quantum information processing and quantum sensing [26–28], with greater than 9 dB of quantum noise reduction demonstrated [29,30]. By transducing the SPR response with quantum noise, we show that the quantum excess noise present when one channel is significantly attenuated, combined with the quantum correlations present in the absence of attenuation, can dramatically improve the SPR sensor sensitivity compared to the analogous classical implementation. In the case of two-mode squeezed states, each individual beam emitted by the 4WM process contains excess quantum noise imparted by the nonlinear amplification. Upon subtraction, the intensities reveal that the excess noise is correlated, and the total noise is reduced below the SNL. If the fields are subtracted with

*pooserrc@ornl.gov

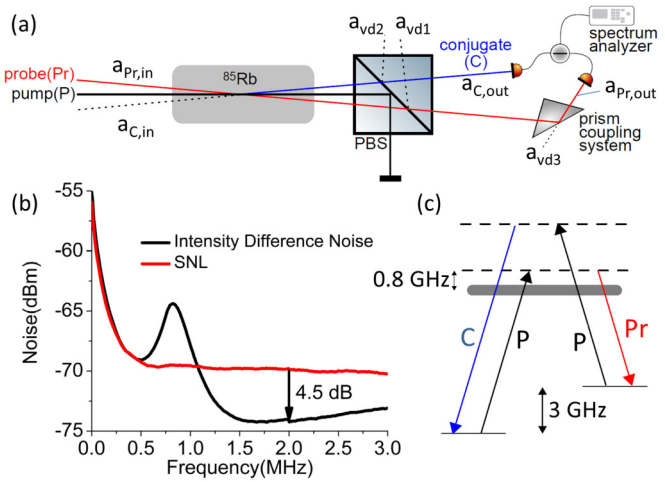

FIG. 1. (Color online) (a) Schematic of the 4WM experiment with the SPR sensing system and the field operators. PBS: polarizing beam splitter. (b) Energy levels of Rb for the $D1$ line at 795 nm, showing that the hot Rb vapor absorbs two pump photons and a correlated probe and conjugate photon pair is reemitted. (c) Broadband squeezing spectrum showing 4.5 dB of squeezing at an analyzer frequency of 2 MHz.

different weights (after one experiences large losses, for instance), then the uncorrelated excess noise on the other field will dominate the signal [31,32].

Figure 1(a) shows the experimental setup used for the quantum Kretschmann configuration SPR sensor. A two-mode squeezed state was generated by 4WM in a 25.4-mm-long ^{85}Rb vapor cell with a 260-mW pump beam and a 77-μW probe beam. The stem of the vapor cell was maintained at 70.3 °C. The pump and probe were fiber coupled to improve the mode quality entering the cell. The 1-mm pump waist and the 0.4-mm probe waist were overlapped at the center of the cell at an angle of 7 mrad. The pump frequency derived from a Ti:sapphire cw laser was locked at ∼795 nm, approximately 800 MHz to the red of the atomic absorption resonance, and the probe frequency was offset from the pump frequency by 3.042 GHz, approximately equal to the hyperfine ground-state splitting, using a double-passed acousto-optic modulator.

The 4WM process is enabled by the double λ system shown in Fig. 1(c). The hot Rb vapor absorbs two pump photons, resulting in a coherence between the two hyperfine ground states. In order to satisfy conservation of energy and momentum, probe and conjugate photon pairs are reemitted simultaneously from the vapor at opposite angles with respect to the pump, which builds quantum correlations between the two channels that can be observed in the form of squeezing in differential measurements. A noise level up to 5 dB below the SNL was observed at an analyzer frequency of 2 MHz in the absence of the SPR sensor. Figure 1(b) shows a typical broadband spectrum with 4.5 dB of quantum noise reduction. The SNL was acquired by measuring the noise of a coherent light source whose power was equal to the sum of the probe power and conjugate powers.

Our SPR sensor based on the Kretschmann configuration used a Borosilicate Crown 7 glass right-angle prism and a 43.5-nm-thick gold film deposited on the long face. Index-matching oils with refractive indices of 1.3 ± 0.0002, 1.301 ± 0.0002, and 1.305 ± 0.0002 were used to characterize the SPR sensor under conditions consistent with flow-cell operation. This resolution was sufficient for this demonstration, but the approach described here could equally well be implemented with any flow-cell geometry. The probe beam was used as the optical transducer as the prism was rotated over an angle of roughly 3° while the conjugate field was sent directly to the balanced photodetector with 94% quantum efficiency.

The classical complex reflection coefficient from the prism-gold film-dielectric multilayer is

$$r = \frac{r_{12} + r_{23}e^{2ik_{z2}d}}{1 + r_{12}r_{23}e^{2ik_{z2}d}}, \tag{1}$$

where r_{ij} is the reflection coefficient between the ith layer and the jth layer, k_{z2} is the normal component of the wave vector in the metal layer, and d is the thickness of the metal film. For p-polarized light, Eq. (1) describes surface plasmon polariton absorption as a function of the incident k vector.

Since the reflectivity of the multilayer depends on the magnitude of k_{z2}, by scanning the angle of incidence an angular reflection spectrum showing an absorption resonance due to the surface plasmon polariton is obtained. When the refractive index of the dielectric changes, so does r_{23}, and therefore the angular spectrum changes. This change is a signal showing that the dielectric has changed in the refractive index.

Treating the readout field quantum mechanically, the total sensor can be described as a parametric amplifier with gain G followed by an effective beam splitter with total transmission η on the probe and conjugate beams before considering the SPR sensor, which can be treated as an effective beam splitter with transmission $\gamma = |r|^2$ for the probe beam. The final probe and conjugate field operators are given by

$$a_{pr_{\text{out}}} = \sqrt{G\eta\gamma}\,a_{pr_{\text{in}}} + \sqrt{(G-1)\eta\gamma}\,a^{\dagger}_{c_{\text{in}}} + \sqrt{(1-\eta)\gamma}\,a_{vd1} + \sqrt{(1-\gamma)}a_{vd3}, \tag{2}$$

$$a_{c_{\text{out}}} = \sqrt{G\eta}a_{c_{\text{in}}} + \sqrt{(G-1)\eta}a^{\dagger}_{p_{\text{in}}} + \sqrt{1-\eta}a_{vd2}. \tag{3}$$

Operators a_{vd1} and a_{vd2} correspond to the input vacuum fields associated with the first beam-splitter port. Operator a_{vd3} corresponds to the input vacuum field associated with the second beam-splitter port. The schematic is shown in Fig. 1(a). The relative intensity noise is given by

$$\Delta N_-^2 = \Delta(a^{\dagger}_{pr_{\text{out}}}a_{pr_{\text{out}}} - a^{\dagger}_{c_{\text{out}}}a_{c_{\text{out}}})^2. \tag{4}$$

For a shot-noise-limited optical state, noise is linearly proportional to optical power. It is therefore possible to perform a direct analog of a typical dc SPR measurement described by Eq. (1) by observing the rf noise on a spectrum analyzer. Doing so can eliminate technical noise sources for SPR sensing at low frequencies (such as laser-amplitude noise or vibration noise) with both classical and quantum optical states and therefore can improve the sensor's resolution. Because of excess laser noise near 1.0 MHz [shown in Fig. 1(c)], the coherent and quantum sensors described here were characterized at 2.0 MHz.

The sensitivity S of an SPR sensor can be described as the product of the sensitivity of the optical readout to SPR

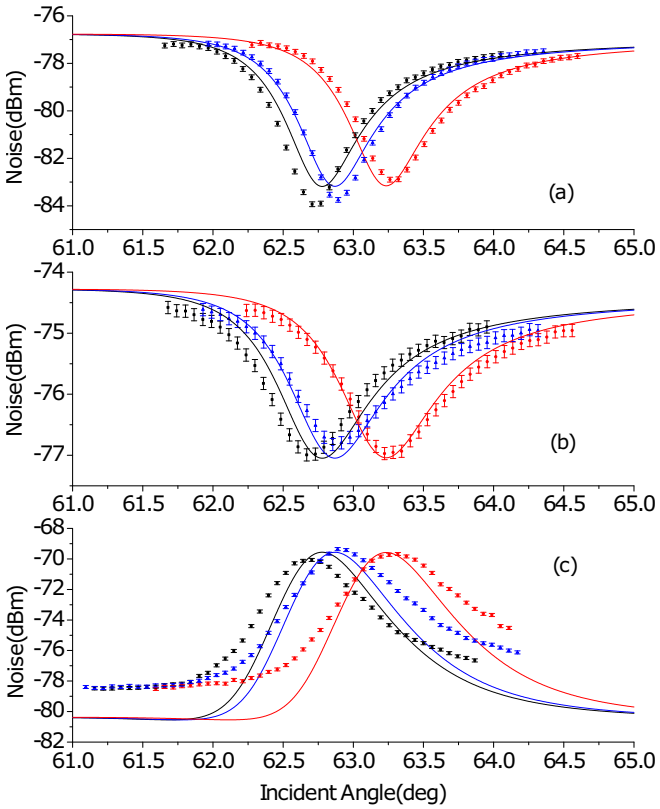

FIG. 2. (Color online) (a) Noise power of the single-channel coherent light source, (b) the noise power of the double-channel coherent light source, and (c) the noise power of the squeezed light source. The simulated noise power is shown by solid lines calculated from the complex reflection coefficient shown in Eq. (1) and the relative intensity noise shown in Eq. (4). The black, blue (dark gray), and red (light gray) lines correspond to a refractive index of 1.3, 1.301, and 1.305. In all cases, the uncertainty in the experimental data was ±0.1 dB statistical and systematic combined error.

absorption and the sensitivity of the surface plasmon itself to changes in local dielectric function:

$$S = \frac{\delta Y}{\delta n_{\mathrm{ef}}} \frac{\delta n_{\mathrm{ef}}}{\delta n}, \tag{5}$$

where Y is the amplitude of the optical signal, n_{ef} is the effective plasmon index, and n is the index of the neighboring dielectric near the metal film [17]. The second factor in Eq. (5) is dependent on the materials properties of the sensor, while the first factor is dependent on the optical readout. Despite a significant breadth of improvements to SPR sensors in recent years, the first factor of Eq. (5) has been fundamentally limited by the photon shot noise. An optical readout method which increases the depth of the modulation on the optical signal would therefore proportionately increase the sensitivity of the SPR sensor.

III. RESULTS AND DISCUSSION

Figure 2(a) illustrates the noise power in the SPR sensor response for the single-channel coherent light source with optical power equal to that of the probe field. The measured noise consists of the sum of shot noise and −84.5 dBm of electronic noise. This signal provides an analog to the current state of the art in classical plasmonic sensing. The modeled data incorporated in Fig. 2(a) are the calculated noise floor ΔN_{pr}^2 using Eq. (1) to determine the transmitted probe intensity. Because the conjugate field functions as a reference for the probe in the quantum sensor and because a reference field is often used to take advantage of common mode rejection in classical shot-noise-limited sensors, a differential classical measurement was also performed. A coherent state with power equal to the combined power of the probe and conjugate fields was split equally on a 50:50 beam splitter with one channel used to transduce the SPR sensor while the other channel served as a reference field. Figure 2(b) illustrates the results of this measurement, while the modeled noise power corresponds to the shot noise for the total transmitted optical power calculated from Eq. (1).

The average depth of the SPR absorption in Fig. 2(b) is 2.3 dB, while the average SPR absorption depth in Fig. 2(a) is 6.4 dB. Since the electronic noise is much weaker than the optical power of the reference channel, the reference channel simply reduces the total modulation strength, as slightly less than half of the combined optical power in Fig. 2(b) is absorbed by the SPR sensor. Note, however, that this would not be the case if the probe field was not shot noise limited, as is true in the vast majority of sensor configurations with optical readout. In that case, excess noise in the probe field would contribute to the signal's dynamic range.

On the other hand, Fig. 2(c) illustrates the noise power for the squeezed light source. As with the classical sensor in Fig. 2(b), the probe field transduces the SPR signal, while the conjugate is used as a reference on the balanced photodetector. Due to the quantum correlations between the probe beam and the conjugate beam, the noise floor off resonance is reduced by 4 dB, equivalent to the amount of squeezing present after the SPR sensor, while uncorrelated quantum noise between the two channels resulting from the attenuation of the probe field by the SPR sensor results in an increase in noise near the SPR resonance. Note that the average magnitude of the SPR absorption in Fig. 2(c) is 8.8 dB, or 2.4 dB better than was possible with a classical state. As described by Eq. (5), an experimental improvement of 2.4 dB in the optical modulation depth corresponds directly to a 2.4-dB improvement in sensitivity. Note that the modeled noise from Eq. (4) plotted in the figure, which represents the noise of a pure squeezed state, suggests that 2 dB of excess noise resulting from unwanted processes in the vapor cell is present in the experimental data off resonance. A pure state would show an even greater improvement of 4.4 dB in absorption depth compared with the classical case. Another viewpoint would be to compare the squeezed state to a classical readout field that is not shot noise limited. In this case, the super-Poissonian noise in the field would serve as an effective modulation. For a modulation commensurate with the amount of antisqueezing present in the two-mode squeezed state, the classical resonance signal would be smaller than the quantum signal by an amount commensurate with the squeezing.

However, the ultimate sensitivity for the quantum measurement is not described by the noise plot but by the measured squeezing [which is itself a normalization of the output noise

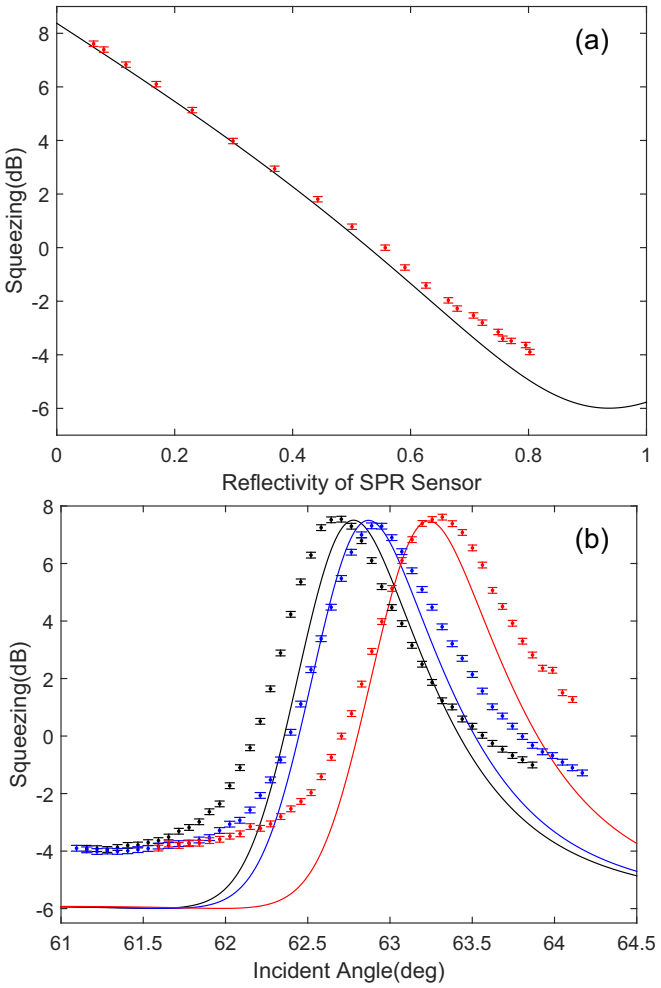

FIG. 3. (Color online) (a) Measured squeezing as a function of the reflectivity of the SPR sensor. (b) Measured squeezing as a function of the incident angle of the SPR sensor. The corresponding simulated relative intensity noise and noise power based on the effective beam-splitter model shown in Eq. (4) are shown as lines. The black, blue (dark gray), and red (light gray) lines correspond to a refractive index of 1.3, 1.301, and 1.305.

by the SNL in Fig. 2(b)]. Figure 3(a) plots the squeezing from Eq. (4) with shot noise subtracted as a function of the reflectivity of the SPR sensor with a gain of $G = 4.5$ and a total transmission of $\eta = 0.84$. The total transmission is the result of 6% attenuation from the vapor cell, 5% attenuation from the polarized beam splitter, and 94% efficiency of the photodetector. The data obtained with the SPR sensor on the probe beam matches well with the model based on the attenuation of quantum correlations by an effective beam splitter except for the high-reflectivity region, which can be accounted for by the fact that the model considers pure states, which our two-mode squeezed state deviates from slightly. The measured and modeled squeezing are illustrated in Fig. 3(b) as a function of incident angle, illustrating an 11.4-dB absorption depth: 5 dB greater than the classical measurement in this configuration. As before, this corresponds directly to a 5-dB improvement in the ultimate sensitivity limit of SPR sensors.

IV. CONCLUSION

Because the absorption depth depends on both quantum correlations when on resonance and quantum anticorrelations when off resonance, this paradigm takes advantage of losses in SPR sensing to enable greater sensitivity with quantum noise measurements than would be possible with an unmodulated signal measurement. As a result, existing squeezed states could be utilized in this framework to support greater than an order of magnitude improved SPR sensitivity in a robust and compact framework that can be easily incorporated with current SPR sensing modalities.

Finally, we note that no proof has yet been developed to show that the approach we demonstrated here will always beat the classical limit, but for the specific sensor developed here, a 5-dB improvement on the classical analog was observed. On the other hand, the absolute sensitivity of our device is in line with the state of the art. Assuming 100 averages for each trace, the error bars correspond to under ± 0.01 dB, which allows for a resolvable index change of 1.7×10^{-6} refractive index unit (RIU) using the reflectivity measured at the inflection point. Our unsqueezed sensor is capable of resolving 2.5×10^{-6} RIU. It is possible to optimize the sensor further by increasing the squeezing in order to beat the state of the art, although we note that in the optimum classical configuration no further increase in SNR can be had. It also stands to reason that with dc measurements, squeezed light would also improve the sensitivity by reducing the variance on each data point in the reflection spectrum, allowing for smaller shifts in the spectrum to become separable as a function of angle. While typical experiments are dominated by technical noise at dc, applying an amplitude modulation at rf frequency to the probe field and then demodulating at this frequency during measurement to measure the amplitude (e.g., via lock-in detection) provide an exact analog to a dc measurement without technical noise. While this dc-equivalent detection scheme will be the subject of a future report, the experimental results presented here demonstrate a clear proof-of-principle improvement in SPR sensors by using quantum noise reduction to increase the modulation depth.

ACKNOWLEDGMENTS

This work was performed at Oak Ridge National Laboratory, operated by UT-Battelle for the U.S. Department of Energy. This paper has been authored by UT-Battelle, LLC, under Contract No. DE-AC05-00OR22725 with the U.S. Department of Energy. The U.S. government retains a nonexclusive, paid-up, irrevocable, worldwide license to publish or reproduce the published form of this paper, or allow others to do so, for U.S. government purposes. The Department of Energy will provide public access to these results of federally sponsored research in accordance with the DOE Public Access Plan. B.L. and R.C.P. acknowledge support from the Laboratory Directed Research and Development program. The gold films used in the SPR sensor were fabricated at the Center for Nanophase Materials Sciences, which is a DOE Office of Science User Facility. The authors acknowledge R. Davidson and J. Schaake for metal deposition support.

[1] C. M. Caves, Phys. Rev. D **23**, 1693 (1981).
[2] F. Wolfgramm, A. Cere, F. A. Beduini, A. Predojević, M. Koschorreck, and M. W. Mitchell, Phys. Rev. Lett. **105**, 053601 (2010).
[3] N. Otterstrom, R. Pooser, and B. Lawrie, Opt. Lett. **39**, 6533 (2014).
[4] J. G. Bohnet, K. C. Cox, M. A. Norcia, J. M. Weiner, Z. Chen, and J. K. Thompson, Nat. Photon. **8**, 731 (2014).
[5] M. A. Taylor, J. Janousek, V. Daria, J. Knittel, B. Hage, H.-A. Bachor, and W. P. Bowen, Nat. Photon. **7**, 229 (2013).
[6] J. Aasi, J. Abadie, B. Abbott, R. Abbott, T. Abbott, M. Abernathy, C. Adams, T. Adams, P. Addesso, R. Adhikari *et al.*, Nat. Photon. **7**, 613 (2013).
[7] R. C. Pooser and B. Lawrie, Optica **2**, 393 (2015).
[8] S. Kawata, Y. Inouye, and P. Verma, Nat. Photon. **3**, 388 (2009).
[9] E. Ozbay, Science **311**, 189 (2006).
[10] C. Lee, M. Tame, J. Lim, and J. Lee, Phys. Rev. A **85**, 063823 (2012).
[11] D. Ballester, M. S. Tame, C. Lee, J. Lee, and M. S. Kim, Phys. Rev. A **79**, 053845 (2009).
[12] E. Kretschmann and H. Raether, Z. Naturforsch. A **23**, 2135 (1968).
[13] J. Homola, S. S. Yee, and G. Gauglitz, Sensors Actuators B **54**, 3 (1999).
[14] K. Matsubara, S. Kawata, and S. Minami, Appl. Opt. **27**, 1160 (1988).
[15] A. V. Kabashin, P. Evans, S. Pastkovsky, W. Hendren, G. A. Wurtz, R. Atkinson, R. Pollard, V. A. Podolskiy, and A. V. Zayats, Nat. Mater. **8**, 867 (2009).
[16] J. N. Anker, W. P. Hall, O. Lyandres, N. C. Shah, J. Zhao, and R. P. V. Duyne, Nat. Mater. **7**, 442 (2008).
[17] M. Piliarik and J. Homola, Opt. Express **17**, 16505 (2009).
[18] S. Y. Wu, H. P. Ho, W. C. Law, C. Lin, and S. K. Kong, Opt. Lett. **29**, 2378 (2004).
[19] A. V. Kabashin, S. Patskovsky, and A. N. Grigorenko, Opt. Express **17**, 21191 (2009).
[20] B. J. Lawrie, P. G. Evans, and R. C. Pooser, Phys. Rev. Lett. **110**, 156802 (2013).
[21] A. Huck, S. Smolka, P. Lodahl, A. S. Sørensen, A. Boltasseva, J. Janousek, and U. L. Andersen, Phys. Rev. Lett. **102**, 246802 (2009).
[22] J. S. Fakonas, H. Lee, Y. A. Kelaita, and H. A. Atwater, Nat. Photon. **8**, 317 (2014).
[23] R. W. Heeres, L. P. Kouwenhoven, and V. Zwiller, Nat. Nanotechnol. **8**, 719 (2013).
[24] D. A. Kalashnikov, Z. Pan, A. I. Kuznetsov, and L. A. Krivitsky, Phys. Rev. X **4**, 011049 (2014).
[25] R. W. Boyd, *Nonlinear Optics*, 3rd ed. (Elsevier, Burlington, MA, 2008).
[26] A. M. Marino, R. C. Pooser, V. Boyer, and P. D. Lett, Nature (London) **457**, 859 (2009).
[27] Y. Cai, J. Feng, H. Wang, G. Ferrini, X. Xu, J. Jing, and N. Treps, Phys. Rev. A **91**, 013843 (2015).
[28] Y. Fang and J. Jing, New J. Phys. **17**, 023027 (2015).
[29] C. F. McCormick, A. M. Marino, V. Boyer, and P. D. Lett, Phys. Rev. A **78**, 043816 (2008).
[30] Q. Glorieux, L. Guidoni, S. Guibal, J.-P. Likforman, and T. Coudreau, Phys. Rev. A **84**, 053826 (2011).
[31] H. A. Bachor and T. C. Ralph, *A Guide to Experiments in Quantum Optics*, 2nd ed. (Wiley-VCH, Weinheim, 2004).
[32] U. Leonhardt, *Measuring the Quantum State of Light* (Cambridge University Press, Cambridge, 2005).